Supernova Neutrino Directionality

Fan Zhang

April 25, 2016

Subject:	Senior Thesis
Date Performed:	Jan 2015 to Apr 2016
Instructor:	Prof. Kate Scholberg
Defense Committee:	Prof. Kate Scholberg
	Prof. Roxanne Springer
	Prof. Seog Oh

Abstract

In this research project, we try to find out how well we can point to core-collapse supernova by detecting supernova neutrino events in a water detector, and to investigate improvement of the pointing algorithm. A refined model is created of supernova neutrinos in which scattered electron events and 30 times more positron events are generated after a burst of supernova neutrinos has propagated through the detector. We tested one old fitting function proposed in 2003 and one new fitting function proposed by us. In most test cases, our model can perform better than the original model.

Contents

1 Introduction

When a massive star comes to the end of its life, it radiates almost all of its energy in the form of neutrinos. While neutrinos come out of the supernova several hours earlier than photons, the detection of neutrinos can give us prompt information about supernova explosion. This information gives an early warning to astronomers about the event, and enables them to detect the details of explosion mechanism of the supernova in early stages. In addition, due to the weak interaction between neutrinos and matter in supernova, detection of supernova neutrinos gives us more insight into the characteristics of the neutrino particle [1].

In this research project, we consider the Super-Kamiokande water Cherenkov detector (See Fig. 1) in Japan to track the neutrino signals. The Super-Kamiokande detector is located 1000 meters underground in Japan, and began to observe on April 1st, 1996. It is operated by an international collaboration of about 110 people and 30 institutes from Japan, the United States, Korea, China, Poland and Spain. The detector consists of a stainless-steel tank, 39 meters in diameter and 42 meter tall, filled with $50\,000$ tons of ultra-pure water, and with about $13\,000$ photomultipliers installed on the tank wall [2].

In the detector, due to the charged-current interaction of neutrinos with water inside the tank, incident neutrinos are converted into relevant charged particles. While the produced products move

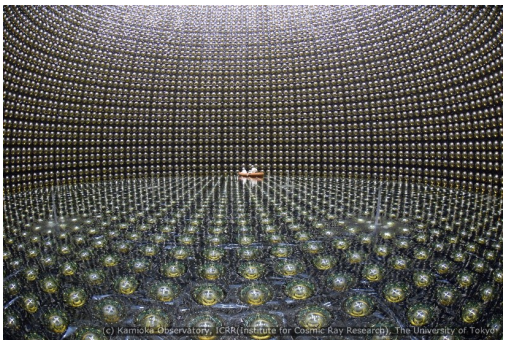

Figure 1: Inner view of Super-Kamiokande detector [5].

faster than the speed of light in water, they will emit shock waves of light - Cherenkov radiation, which could be detected by the photomultiplier tubes [3]. By measuring the Cherenkov ring produced and using the timing and charge information recorded by photomultiplier tubes on the wall, the interaction vertex, ring direction and flavor of incident neutrinos can be reconstructed. These data will give us the direction information we need. A generated Cherenkov ring from incident neutrino is illustrated in Fig. 2.

Until now, the expected pointing ability of Super-Kamiokande is about 8°, which can be improved

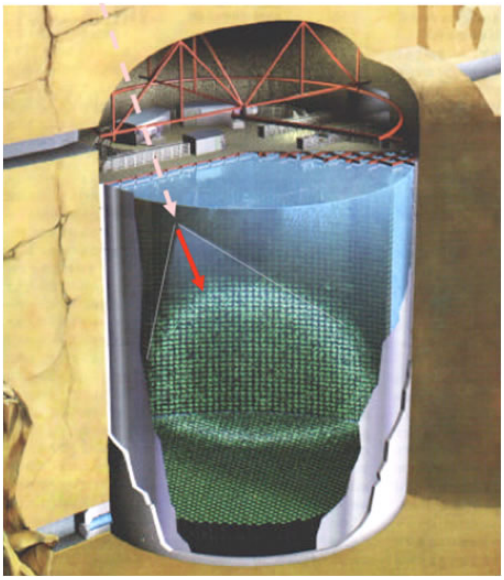

Figure 2: An incident neutrino will generate Cherenkov ring while interacting with media in the detector.

to 3° with good tagging, and even better by the virtue of much larger statistics[4]. However, better accuracy is desirable to enable fast detection of the supernova.

Also taking into consideration that future construction of Hyper – Kamiokande detector (which is the next generation neutrino detector, more than 10 times larger than current Super-Kamiokande

detector [6]) requires well-proven technology and higher ability to infer neutrino interaction location to its incident angle, we need to further improve our ability to locate supernova directly.

2 Research Process

Our research purpose is to find out how well we can point to supernovae by detecting supernovae neutrino events in a water detector, and to investigate improvement of the pointing algorithm. This improvement on directionality would help scientists to locate supernovae more accurately.
The research procedure was:

1. First, we built a refined model of supernova neutrinos in which scattered electron events and 30 times more positron events are generated after a burst of supernova neutrinos has propagated through the detector. We used this model to generate data and to test our algorithm.

2. Then, simulated events were generated via Monte Carlo from this supernova model to provide signals which are supposed to be detected in a supernova neutrino burst. Then, we extracted probability density functions from these signals to build our fitting function.

3. Finally, we tested both one fitting function proposed in 2003 and our function, to determine whether our model can increase the pointing efficiency for locating supernova locations.

3 Supernova neutrino model

If a supernova burst has occurred, its neutrinos will propagate into the detector and generate some electron events and approximately 30 times the number of positron events. The electron events come from elastic scattering between neutrino and electrons, while positron events are generated from inverse beta decay.

3.1 Neutrino energy distribution

The out-burst supernova neutrinos possess a spectrum of energy distribution. Among all the models of expected supernova neutrino energy spectra, we adopted the GVKM model[7], which is shown in Fig. 3.

For each incoming neutrino, we'll use Monte Carlo method to calculate its energy according to the energy spectrum. Then, in the following two sections, we will discuss how to generate electron or positron events using incoming neutrino's information.

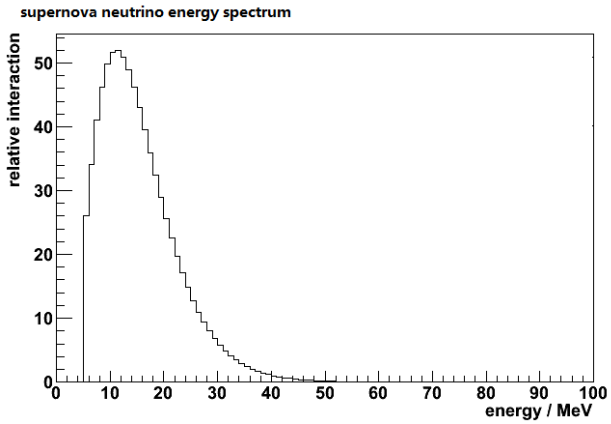

Figure 3: Expected supernova anti-electron neutrino energy spectrum.

3.2 Electron events from elastic scattering

Low energy electron neutrinos can be detected via $\nu + e^- \rightarrow \nu + e^-$ elastic scattering. The kinetic energy distribution of recoil electron as a function of neutrino energy E_ν is given by [9]

$$\frac{d\delta(T, E_\nu)}{dT} = \frac{2G_F^2 m_e}{\pi}[A^2 + B^2(1 - \frac{T}{E_\nu})^2 - AB\frac{m_e T}{(E_\nu)^2}]$$

where m_e is the electron mass, T is the kinetic energy of the recoil electron and G_F is Fermi constant. And A and B are also given in this paper.
In addition, the energy of recoil electron is also related to its scattering angle θ by

$$T = m_e \frac{2\cos^2\theta}{(1 + m_e/E_\nu)^2 - \cos^2\theta}$$

where θ is the recoil electron scattering angle with respect to the incoming neutrino's direction.
Thus, with these two functions, given one neutrino direction and its energy, we can obtain a distribution of its recoil electron's recoil angle and kinetic energy. For example, the distribution of recoil electron's recoil angle is shown in Fig. 4, where the neutrino energy is 30 MeV, and the x-axis is the cosine value of angle between recoil direction and true direction. It can be seen from the distribution of recoil angle that direction information from electron events can be used as a significant source of pointing information to estimate the incoming neutrino's direction.

3.3 Positron events from inverse beta decay

In addition, positron events are also generated in the detector through inverse beta decay, where electron anti-neutrinos are scattered off from protons via

$$\bar{\nu_e} + p \rightarrow e^+ + n$$

The cross section can also be calculated from reference [10]. With details omitted, two points shall be noticed:

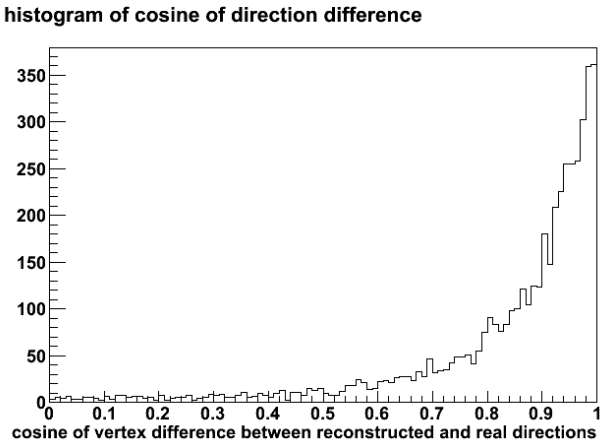

Figure 4: Histogram of cosine value of angle between recoil electron's direction and neutrino's direction, when neutrino energy is 30 MeV.

First, the number of positron events are about 30 times the number of electron events. This means that, for each electron event signal detected in the detector, there will also be 30 positron events detected simultaneously which barely have pointing information. Such isotropic background will make it much more difficult to estimate the incoming neutrino's direction.
Second, the distribution of positron events varies with the incoming neutrino energy. If the incoming neutrino energy is less than 15 MeV, the positron distribution would lean a little backward (opposite direction from neutrino's), while it will lean slightly forward when energy is larger than 15 MeV. For example, the histograms of recoil angles between positron and neutrino for energies is in different ranges are shown in Fig. 5 ($E_\nu < 10$ MeV), Fig. 6 ($10 < E_\nu < 15$ MeV), Fig. 7 ($15 < E_\nu < 22$ MeV), Fig. 8 ($22 < E_\nu < 35$ MeV), Fig. 9 ($E_\nu > 35$ MeV), where the x-axis is cosine of recoil angle. If the cosine of the angle is approaching 1, the electron direction is closer to the incoming neutrino direction. It can be seen that the distribution does vary a lot according to the incoming neutrino energy. So we can also use this leaning information to estimate the incoming neutrino direction, in order to help locate the supernova.

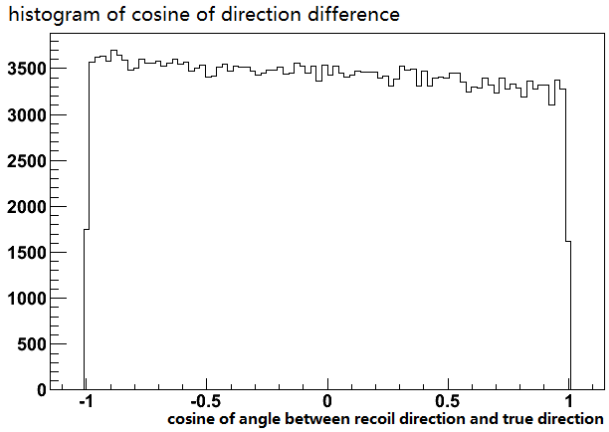

Figure 5: Histogram of positron recoil angle with respect to true direction, when neutrino energy is less than 10 MeV.

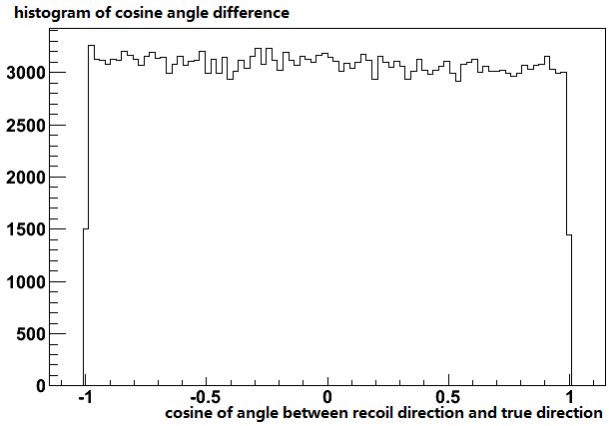

Figure 6: Histogram of positron recoil angle with respect to true direction, when neutrino energy is between 10 MeV and 15 MeV.

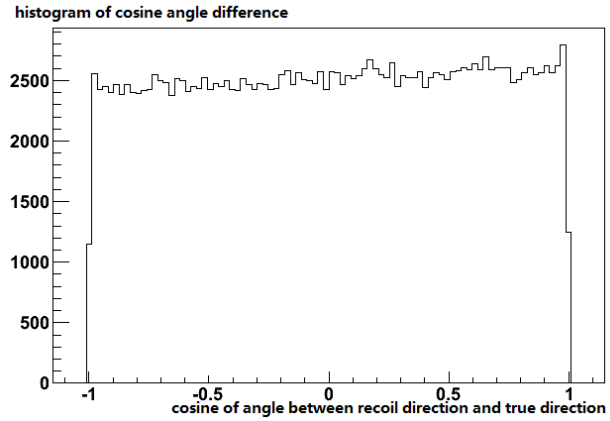

Figure 7: Histogram of positron recoil angle with respect to true direction, when neutrino energy is between 15 MeV and 22 MeV.

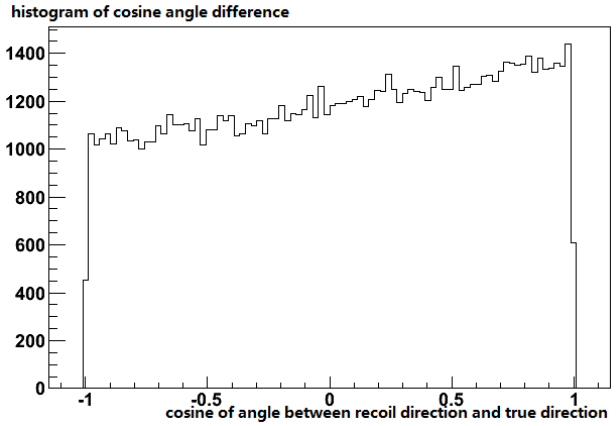

Figure 8: Histogram of positron recoil angle with respect to true direction, when neutrino energy is between 22 MeV and 35 MeV.

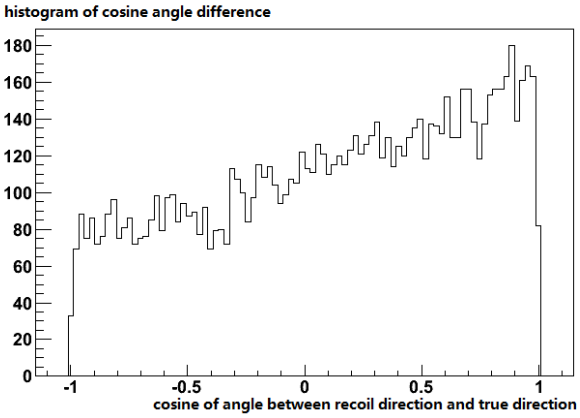

Figure 9: Histogram of positron recoil angle with respect to true direction, when neutrino energy is larger than 35 MeV.

4 Simulated detector signals

Our supernova model consists of electron events from elastic scattering and positron events from inverse beta decay. The electron events can point more directly to supernova, so they serve as the main pointing information. In contrast, positron events can barely point to supernova, and they act more as background events. Then we simulate supernova neutrino products in the detector, and output corresponding data that can be used to estimate incoming neutrino direction - θ and ϕ.
Theoretically, if we can separate electron events from positron events, the two-dimensional plot of pointing information (θ vs ϕ) will be like Fig. 10. When the electron events and positron events are denoted clearly by color using Monte Carlo truth, it's very easy to tell the incoming neutrino direction from the red dots.

However, in real detector signals, we cannot separate the electron events from positron events.

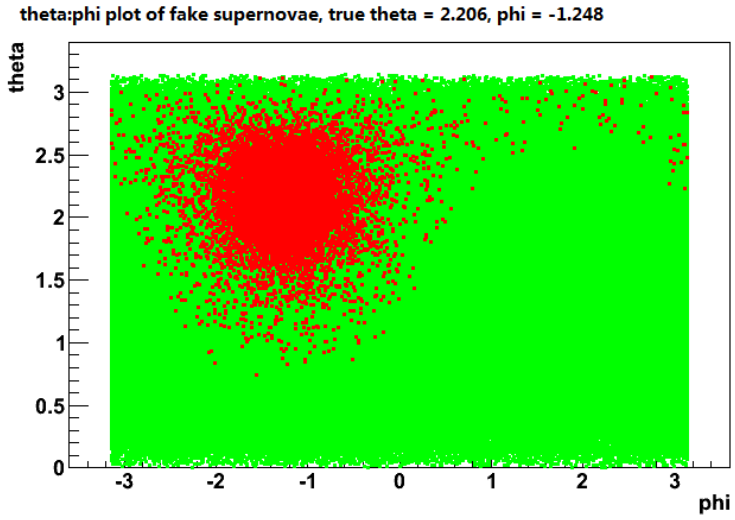

Figure 10: theta:phi plot for both electron and positron events. The red dots refer to electron events, which can point to supernovae. The green dots are positron events, 30 times more than electron events but nearly isotropic, acting primarily as background.

The real direction plot (θ vs ϕ) of supernova signals should look like Fig. 11. This graph is messy, and it's much more difficult to locate the peak.

In order to find out the peak of direction plots, we make a contour plot of data (Fig. 12). If we can find a function $f(\theta, \phi)$ which fits the shape of this plot best, we can easily determine the peak of this direction plot. But, it's still a little difficult to guess a two dimensional function with two variables - θ and ϕ.

We suppose, for each point whose distance from the peak is x, their heights in the plot are the same. Then, we can reduce a two-dimensional function $f(\theta, \phi)$ into a one-dimensional function $f(x)$, which only depends on the points' distances to the peak. (An illustration is demonstrated in Fig. 13).

In the plot, x is the distance between any point (θ, ϕ) and the peak point (θ_0, ϕ_0). In reality, x

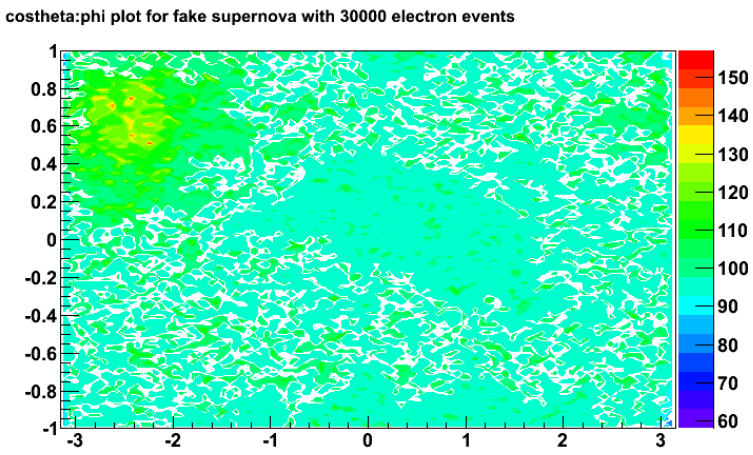

Figure 11: costheta:phi plot for electron and positron events. The redder the color, the denser the plot. Our task is to locate the most dense point in the plot. True theta = 0.849, phi = -2.478.

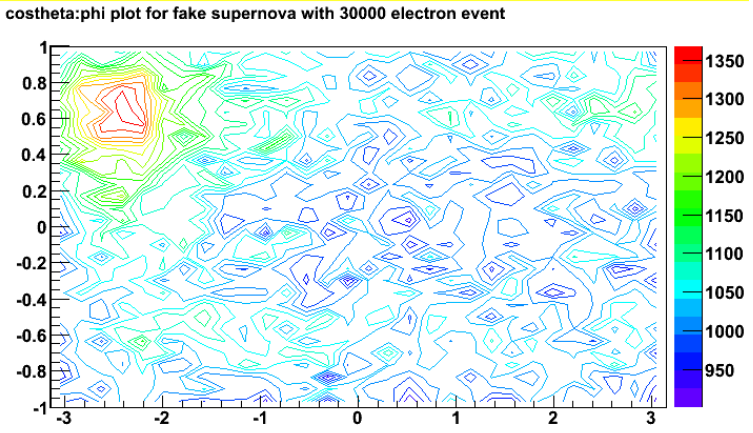

Figure 12: Contour plot of pointing information, costheta vs phi. Same true direction as Fig. 11.

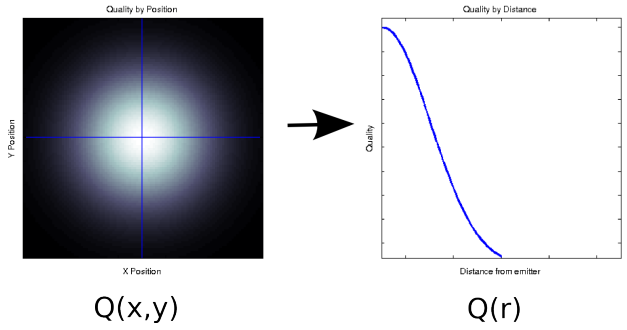

Figure 13: Illustration of dimension reduction - collapse a two-dimensional graph into a one-dimensional histogram radially.

represents the cosine value of angle between one direction (can be mapped to (θ, ϕ) in the plot) and the true direction of the supernovae (peak point (θ_0, ϕ_0) in the plot). Thus, x can be calculated to be

$$\begin{aligned} x &= x_1 \cdot x_0 + y_1 \cdot y_0 + z_1 \cdot z_0 \\ &= \cos\phi \sin\theta \cdot \cos\phi_0 \sin\theta_0 + \sin\phi \sin\theta \cdot \sin\phi_0 \sin\theta_0 + \cos\theta \cdot \cos\theta_0 \\ &= \cos\theta \cos\theta_0 + \sin\theta \sin\theta_0 (\cos\phi \cos\phi_0 + \sin\phi \sin\phi_0) \\ &= \cos\theta \cos\theta_0 + \sin\theta \sin\theta_0 \cos(\phi - \phi_0) \end{aligned}$$

With this trick, the problem can be reduced to: how could we find a best estimation of $f(x)$?

5 Algorithm improvement

In the above section, we have reduced our research problem to: How to find a best estimation of $f(x)$ that fits the supernova direction plots best?
With the reduction of two variables θ, ϕ to one variable x, we have also reduced our supernova direction costheta:phi plot into a one-dimensional histogram of x, as in Fig. 14 (where according to the definition of angle difference, $x = 1$ means two directions are the same as each other).
This graph looks like a combination of one exponential function and one constant.

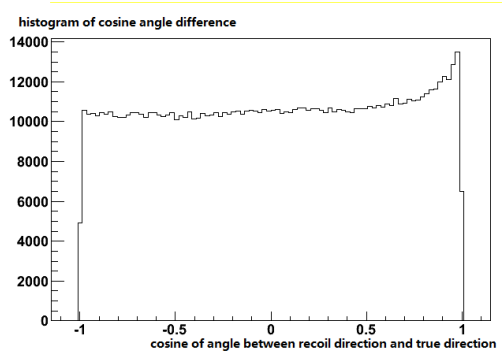

Figure 14: We use electron and positron distributions to build our supernovae model, and use it to create the plot of direction difference between detected event directions and the true direction.

5.1 Tomas model

This graph does look like one exponential function plus one constant. In 2003, Tomas has given his function for this plot [8]

$$f(\theta, \phi|\theta_0, \phi_0)d\theta d\phi = \frac{d\mu}{N_b + N_s}[\frac{N_b}{4\pi} + \frac{N_s}{C} \cdot \exp(-\frac{\ell^2}{2\delta_s^2})]$$

where

$$\ell = \arccos(\cos\theta + \cos\theta_0 + \sin\theta \sin\theta_0 \cos(\phi - \phi_0))$$

In our case, with constants calculated, the function becomes

$$f_{tomas}(x) = \frac{d\mu}{N_b + N_s}[\frac{N_b}{4\pi} + \frac{N_s}{C} \cdot \exp(-\frac{\arccos^2(x)}{2\delta_s^2})]$$

However, this function can be improved to better model the data.

5.2 Our model

Although the positron background distribution in the one-dimensional histogram (Fig. 14) looks like a constant, and it's considered as $\frac{N_b}{4\pi\cdot(N_b+N_s)}$ in Tomas's function, it's actually not. As we have discussed in Section 2, the distribution varies according to incoming neutrino's direction.
So if we separate positron events into different energy channels, and add them together according to their weight, this function will fit better to the direction distribution, which will output a better estimation of the peak.
So we set it to be a combination of distribution functions of different energy bins i

$$f_{positron}(x) = \sum_i f_i(x)$$

Similarly, we will also apply this algorithm to electron scattering events. Currently we set bin number to be 5, so the total probability density function (pdf) of histogram $f(x)$ becomes a combination of 5 electron pdf and 5 positron pdf. An example of electron events in different bins is shown in Fig. 15, while an example of positron events in different bins is shown in Fig. 16.
So, in our research, we first generated data from our supernova model, then extracted parameters for different electron and positron bins. Then, we combine them into one combined function $f(x)$, and use this function to get our estimation of supernova's location.

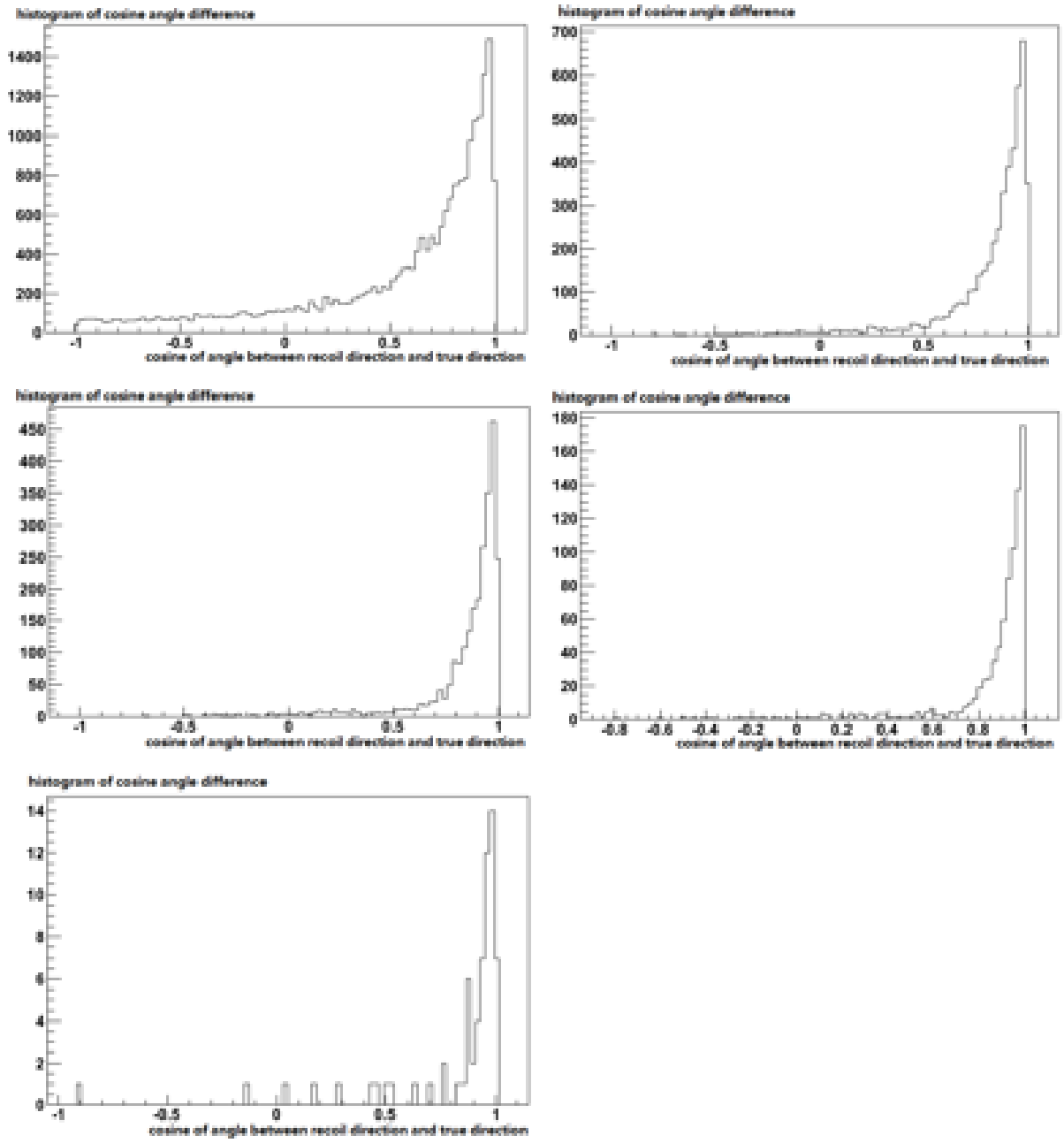

Figure 15: In this graph, the electron events in one supernovae event are divided into 5 bins according to energy. From left to right, they are 0 - 10, 10 - 15, 15 - 22, 22 - 35, 35 - MeV. The shape of histograms varies a little among energy bins.

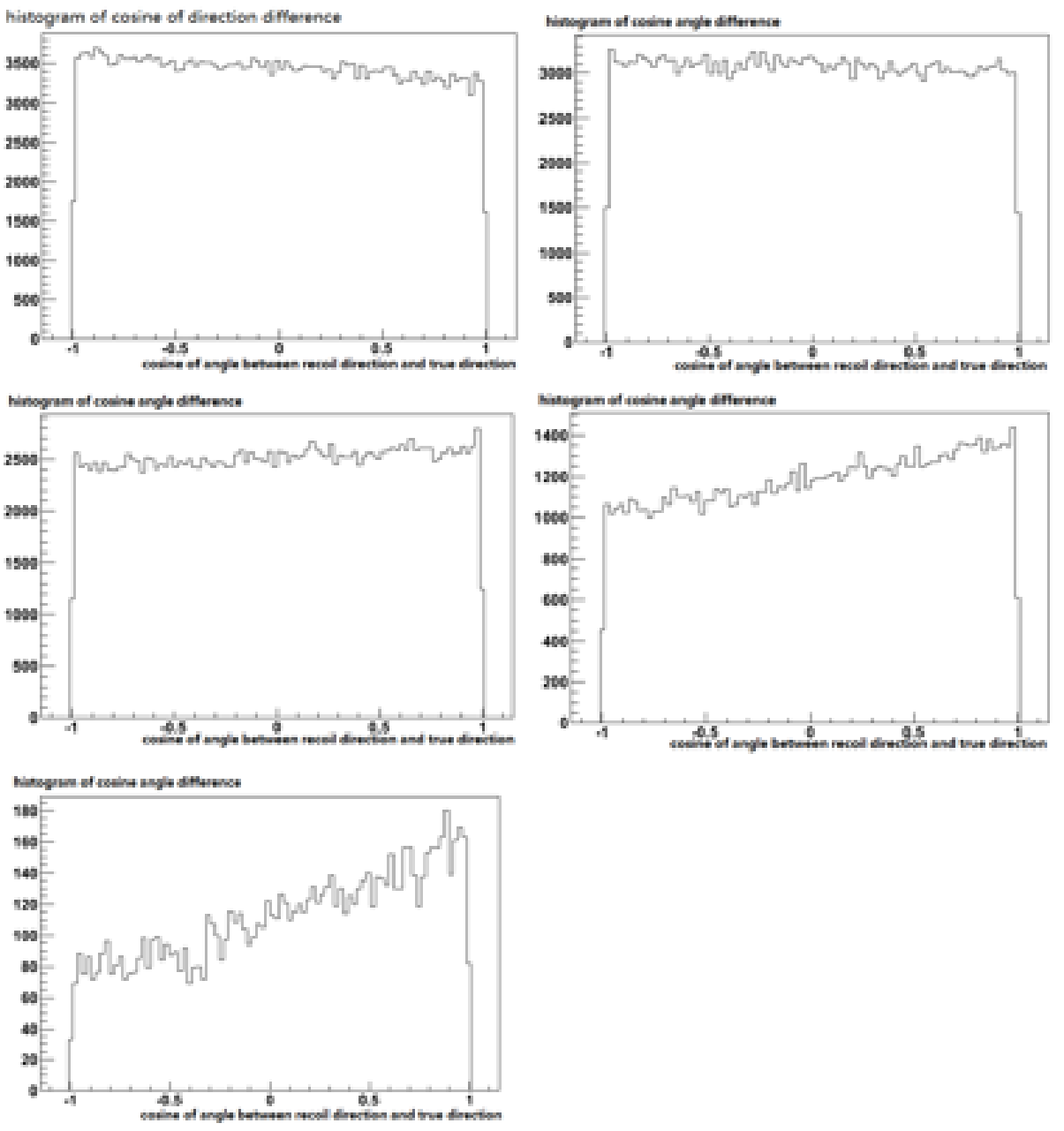

Figure 16: In this graph, the positron events are divided into 5 bins according to energy. From left to right, they are 0 - 10, 10 - 15, 15 - 22, 22 - 35, 35 - MeV. The shape of histograms vary a little according to different energy bins.

6 Result

6.1 Example of Estimation Process

Before we tested our algorithm, we first made a test using Tomas' model. We used his function to fit to one fake supernova event with 30000 neutrinos from one direction, whose true direction is $\theta = 0.849, \phi = -2.478$ (units in radians). His estimation of incoming neutrino's direction is $\theta' = 0.881, \phi' = -2.426$ (units in radians), which only has a 0.051 radian angle difference from the true direction.

Then, we tried to test our algorithm. For the positron distributions, we set their probability density functions (pdf) to be in the form of $A \cdot x + B$ because currently we couldn't find other functions which can fit better. For the electron distributions, we tried several candidates.

Our estimations of the incoming direction for this same supernova true direction are recorded in Tab. 6.1. It can be seen from this table that, the fitting result only changes a little according to different choices of electron pdf. But, if we define pointing efficiency as cosine value of angle between estimated direction and true direction, then our estimate can improve the pointing efficiency by 45% in this test case.

Table 1: Table of estimate based on Tomas' function and our estimate of the incoming neutrino direction of fake supernova No.1 with 30000 neutrino events.

electron pdf	positron pdf	θ	ϕ	angle diff
True	True	0.849	-2.478	/
Tomas	Tomas	0.8816 ± 0.0071	-2.4262 ± 0.0093	$0.0511 \pm 0.89\%$
$A \cdot \exp(B \cdot x) + C$	$A \cdot x + B$	0.8674 ± 0.0113	-2.4508 ± 0.0152	$0.0276 \pm 1.44\%$
$\sum_{i=1}^{2} A_i \cdot \exp(B_i \cdot x) + C$	$A \cdot x + B$	0.8682 ± 0.0110	-2.4517 ± 0.0150	$0.0276 \pm 1.41\%$
$\sum_{i=1}^{3} A_i \cdot \exp(B_i \cdot x) + C$	$A \cdot x + B$	0.8681 ± 0.0110	-2.4516 ± 0.0149	$0.0276 \pm 1.41\%$
$\sum_{i=1}^{4} A_i \cdot \exp(B_i \cdot x)$	$A \cdot x + B$	0.8680 ± 0.0109	-2.4515 ± 0.0149	$0.0276 \pm 1.40\ \%$

6.2 All results

Similarly, we applied this estimation process to some other fake supernova event with different number of incoming neutrinos. The tables of estimate based on Tomas' function and our estimates are recorded in the following tables. (Because the estimation results are very similar for different electron probability density functions, here we only recorded the results with electron pdf in the form of $\sum_{i=1}^{4} A_i \cdot \exp(B_i \cdot x)$.)

For 3 fake supernova event with 30000 neutrinos, their table are Tab. 6.1, Tab. 6.2 and Tab. 6.2.
For 3 fake supernova event with 3000 neutrinos, their table are Tab. 6.2, Tab. 6.2 and Tab. 6.2.
For 3 fake supernova event with 1000 neutrinos, their table are Tab. 6.2, Tab. 6.2 and Tab. 6.2.
For 3 fake supernova event with 200 neutrinos, their table are Tab. 6.2, Tab. 6.2 and Tab. 6.2.

Table 2: Table of estimate based on Tomas' function and our estimate of the incoming neutrino direction of fake supernova No.2 with 30000 neutrino events.

electron pdf	positron pdf	θ	ϕ	angle diff
True	True	1.903	-0.682	/
Tomas	Tomas	1.9510 ± 0.0078	-0.6899 ± 0.0081	$0.0486 \pm 1.24\ \%$
$\sum_{i=1}^{4} A_i \cdot \exp(B_i \cdot x)$	$A \cdot x + B$	1.9371 ± 0.0118	-0.7030 ± 0.0122	$0.0394 \pm 1.84\%$

Table 3: Table of estimate based on Tomas' function and our estimate of the incoming neutrino direction of fake supernova No.3 with 30000 neutrino events.

electron pdf	positron pdf	θ	ϕ	angle diff
True	True	0.660	0.221	/
Tomas	Tomas	0.6514 ± 0.0072	0.2082 ± 0.0127	$0.0116 \pm 6.20\%$
$\sum_{i=1}^{4} A_i \cdot \exp(B_i \cdot x)$	$A \cdot x + B$	0.6336 ± 0.0110	0.1976 ± 0.0197	$0.0299 \pm 10.12\%$

Table 4: Table of estimate based on Tomas' function and our estimate of the incoming neutrino direction of fake supernova No.4 with 3000 neutrino events.

electron pdf	positron pdf	θ	ϕ	angle diff
True	True	1.1162	0.6295	/
Tomas	Tomas	1.0218 ± 0.0227	0.6117 ± 0.0283	$0.0957 \pm 5.13\%$
$\sum_{i=1}^{4} A_i \cdot \exp(B_i \cdot x)$	$A \cdot x + B$	1.0243 ± 0.0348	0.6207 ± 0.0427	$0.0922 \pm 7.67\%$

Table 5: Table of estimate based on Tomas' function and our estimate of the incoming neutrino direction of fake supernova No.5 with 3000 neutrino events.

electron pdf	positron pdf	θ	ϕ	angle diff
True	True	2.3781	1.0494	/
Tomas	Tomas	2.3039 ± 0.0223	1.1167 ± 0.0372	$0.0885 \pm 3.47\%$
$\sum_{i=1}^{4} A_i \cdot \exp(B_i \cdot x)$	$A \cdot x + B$	2.3214 ± 0.0346	1.1265 ± 0.0532	$0.0789 \pm 4.95\%$

Table 6: Table of estimate based on Tomas' function and our estimate of the incoming neutrino direction of fake supernova No.6 with 3000 neutrino events.

electron pdf	positron pdf	θ	ϕ	angle diff
True	True	1.3428	-2.0354	/
Tomas	Tomas	1.2865 ± 0.0244	-2.0345 ± 0.0254	$0.0563 \pm 2.27\%$
$\sum_{i=1}^{4} A_i \cdot \exp(B_i \cdot x)$	$A \cdot x + B$	1.3035 ± 0.0365	-2.0415 ± 0.0382	$0.0397 \pm 3.37\%$

Table 7: Table of estimate based on Tomas' function and our estimate of the incoming neutrino direction of fake supernova No.7 with 1000 neutrino events.

electron pdf	positron pdf	θ	ϕ	angle diff
True	True	1.1242	2.5812	/
Tomas	Tomas	1.3969 ± 1.6106	0.1349 ± 0.7719	FAIL
$\sum_{i=1}^{4} A_i \cdot \exp(B_i \cdot x)$	$A \cdot x + B$	3.1500 ± 0.0276	0.0849 ± 2.3792	FAIL

Table 8: Table of estimate based on Tomas' function and our estimate of the incoming neutrino direction of fake supernova No.8 with 1000 neutrino events.

electron pdf	positron pdf	θ	ϕ	angle diff
True	True	1.9315	-2.3950	/
Tomas	Tomas	1.9446 ± 0.0468	-2.3338 ± 0.0530	$0.0586 \pm 3.31\%$
$\sum_{i=1}^{4} A_i \cdot \exp(B_i \cdot x)$	$A \cdot x + B$	1.9244 ± 0.0641	-2.3125 ± 0.0741	$0.0776 \pm 4.62\%$

Table 9: Table of estimate based on Tomas' function and our estimate of the incoming neutrino direction of fake supernova No.9 with 1000 neutrino events.

electron pdf	positron pdf	θ	ϕ	angle diff
True	True	0.3528	-1.9601	/
Tomas	Tomas	0.2976 ± 0.0411	-2.1847 ± 0.1338	$0.0902 \pm 15.11\%$
$\sum_{i=1}^{4} A_i \cdot \exp(B_i \cdot x)$	$A \cdot x + B$	0.3012 ± 0.0633	-2.1078 ± 0.2126	$0.0699 \pm 23.31\%$

Table 10: Table of estimate based on Tomas' function and our estimate of the incoming neutrino direction of fake supernova No.10 with 200 neutrino events.

electron pdf	positron pdf	θ	ϕ	angle diff
True	True	0.4049	1.3793	/
Tomas	Tomas	1.6500 ± 0.1102	-0.5182 ± 0.0824	FAIL
$\sum_{i=1}^{4} A_i \cdot \exp(B_i \cdot x)$	$A \cdot x + B$	0.3814 ± 0.1080	0.8658 ± 0.3145	$0.1962 \pm 46.06\%$

Table 11: Table of estimate based on Tomas' function and our estimate of the incoming neutrino direction of fake supernova No.11 with 200 neutrino events.

electron pdf	positron pdf	θ	ϕ	angle diff
True	True	2.7134	-0.7035	/
Tomas	Tomas	0.9081 ± 0.1201	0.2932 ± 0.1264	FAIL
$\sum_{i=1}^{4} A_i \cdot \exp(B_i \cdot x)$	$A \cdot x + B$	0.7283 ± 0.2816	0.3833 ± 0.3119	FAIL

Table 12: Table of estimate based on Tomas' function and our estimate of the incoming neutrino direction of fake supernova No.12 with 200 neutrino events.

electron pdf	positron pdf	θ	ϕ	angle diff
True	True	2.4415	0.7258	/
Tomas	Tomas	2.8075 $\pm$ 2.7128	1.0966 $\pm$ 5.0654	0.4042 $\pm$ 471.92%
$\sum_{i=1}^{4} A_i \cdot \exp(B_i \cdot x)$	$A \cdot x + B$	3.1500 $\pm$ 0.0678	-1.3482 $\pm$ 3.9949	FAIL

7 Conclusion

In this research, we have built a refined model of supernova neutrinos where scattered electron events and 30 times more positron events are generated after a beam of supernova neutrinos have propagated through the detector from one single direction. In ideal supernova cases with a large number of neutrino events, our model can perform better than Tomas model. However, because the number of test cases is not large enough, we need further study.
These are factors which we need to conduct further research on that may increase pointing accuracy:

1. Positron pdf. In current tests, we set the positron pdf to be $A \cdot x + B$. Although functions such as $A \cdot x^2 + B$ or $A \exp(B \cdot x) + C$ doesn't fit well with the histogram, a better model for the positron pdf might improve our pointing accuracy.

2. Different energy channels. Currently we only have 5 energy bins: $< 10, 10 - 15, 15 - 22, 22 - 35, > 35$ MeV, but increasing energy channels is supposed to improve the pointing accuracy.

3. Test model on other supernova samples from more directions.

4. Test model on argon detectors.

So, further research needs to be conducted to improve the efficiency of this algorithm.

8 Reference

References

[1] The Elusive Neutrino, by Nickolas Solomey

[2] Super-Kamiokande official website, http://www-sk.icrr.u-tokyo.ac.jp/sk/about/intro-e.html

[3] The Super-Kamiokande detector, by the Super-Kamiokande collaboration, http://www-sk.icrr.u-tokyo.ac.jp/doc/sk/pub/sknimpaper.pdf

[4] Supernovae neutrino detection, by Kate Scholberg, arXiv:1205.6003 [astro-ph.IM].

[5] Inner view of Super-Kamiokande: http://www-sk.icrr.u-tokyo.ac.jp/sk/gallery/wme/PH20-water-withboat-apr23-wm.jpg

[6] The Hyper-Kamiokande experiment – Detector Design and Physics Potential, arXiv:1109.3262 [hep-ex]

[7] Supernova Neutrino Detection - Scholberg, Kate, Ann.Rev.Nucl.Part.Sci. 62 (2012) 81-103 arXiv:1205.6003 [astro-ph.IM]

[8] Supernova pointing with low- and high-energy neutrino detectors, Phys.Rev. D68 (2003) 093013

[9] Determining the Flavour Content of the Low-Energy Solar Neutrino Flux, JHEP 0008:025,2000

[10] Precise quasielastic neutrino/nucleon cross section, Phys.Lett.B564:42-54,2003